

Multiband superconductivity due to the electron - LO-phonon interaction in strontium titanate and on a SrTiO₃/LaAlO₃ interface

S. N. Klimin · J. Tempere · J. T. Devreese · D. van der Marel

Received: date / Accepted: date

Abstract In strontium titanate, the Fröhlich electron - LO-phonon interaction dominates the electron response and can also provide superconductivity. Because of high LO-phonon frequencies in SrTiO₃, the superconducting system is non-adiabatic. We demonstrate that the dielectric function approach is an adequate theoretical method for superconductivity in SrTiO₃ and on the SrTiO₃-LaAlO₃ interface. The critical temperatures are calculated using realistic material parameters. The obtained critical temperatures are in line with experimental data both for bulk and interface superconductivity. The present method explains the observed multidome shape of the critical temperature in SrTiO₃ as a function of the electron concentration due to multiband superconductivity.

Keywords Superconductivity · Strontium titanate · Interface

1 Introduction

The discovery of a highly conducting two-dimensional electron gas at the interface between two insulators, SrTiO₃ and LaAlO₃ [1] stimulated intense experimental and theoretical studies which led to the observa-

tion of fascinating phenomena such as superconductivity [2,3,4,5,6] coexisting with ferromagnetism [7,8,9] and spin-orbit coupling [10,11]. These effects are related to unique properties of strontium titanate. The superconducting phase transition in strontium titanate and on SrTiO₃-based interfaces occurs at low temperatures combined with low carrier densities, so that it was called “the most dilute superconductor” [12]. Recent experimental studies demonstrated the possibility to control parameters of the electron gas at the LaAlO₃/SrTiO₃ interface by an external electric field [3,4,5,6]. In particular, this allow to study the dependence of the superconducting transition temperature on the electron concentration. Consequently, these investigations have reopened the discussion about the mechanism of superconductivity in bulk strontium titanate.

SrTiO₃ is a strongly polar crystal. Therefore the Fröhlich electron - LO-phonon interaction dominates in the electron response of SrTiO₃ [13], and the phonon-mediated electron-electron attraction is considered as a likely candidate to provide superconductivity in strontium titanate [14,15,16,17].

Because the LO-phonon frequencies are high with respect to both the thermal energy and the Fermi energy, the superconducting system is strongly non-adiabatic. The adequate theoretical method for superconductivity in the non-adiabatic electron - LO-phonon system is the dielectric function approach [15,18,19]. We apply the dielectric function approach as a unique method to treat superconductivity both at the SrTiO₃-LaAlO₃ interface [16] and in bulk doped strontium titanate. This study is performed using recent results for the band structure of SrTiO₃ [20,21,22]. The critical temperatures are calculated without fitting. For the calculations, we use well-established material parameters, except for the acoustic deformation potential of stron-

S. N. Klimin · J. Tempere · J. T. Devreese
Theorie van Kwantumsystemen en Complexe Systemen (TQC), Universiteit Antwerpen, Universiteitsplein 1, BE-2610 Antwerpen, Belgium
E-mail: sergei.klimin@uantwerpen.be

J. Tempere
Lyman Laboratory of Physics, Harvard University, Cambridge, Massachusetts 02138, USA

D. van der Marel
Département de Physique de la Matière Condensée, Université de Genève, CH-1211 Genève 4, Switzerland

tium titanate, for which the values reported in the literature show a considerable spread [23,24]. The calculated critical temperatures are compared with available experimental data.

2 Superconductivity in complex oxides and their interfaces within the dielectric function method

In view of recent discussions, it is relevant to revisit the theoretical treatment of superconductivity in bulk strontium titanate. There exist different approaches to treat the superconductivity in polar crystals due to the electron – LO-phonon interaction, see, e. g., Refs. [14, 15, 16, 17, 18]. In the present work, the superconducting transition temperatures in n -doped SrTiO₃ are calculated within the dielectric function approach [18, 15, 19]. We can recalculate the critical temperatures in bulk strontium titanate using the dielectric function method accounting for the most recent results [20, 21, 22] on the band structure and optical-phonon spectrum of strontium titanate.

Recently, an alternative approach for the description of superconductivity in complex oxides and their interfaces has been developed in Refs. [17, 28]. It is stated in these works that the electron-electron interaction mediated by the LO phonons is sufficient to overcome the Coulomb repulsion in strontium titanate and can lead therefore to an effective attraction potential. This question requires careful analysis. Below, we argue that the approach of [17, 28] in which the LO-phonon mediated electron-electron interaction relates to the static dielectric constant is insufficient to describe superconductivity in strontium titanate.

The matrix element for the effective electron-electron interaction provided by phonons is modeled in Ref. [17] by a two-particle potential in the Bardeen – Pines form [29], which for a single-mode polar crystal is given by:

$$\Gamma(\mathbf{p}, E_n | \mathbf{k}, E_m) = \frac{4\pi e^2}{\varepsilon_\infty q^2} - \frac{2\omega_L |V_{\mathbf{q}}|^2}{\omega_L^2 + (E_n - E_m)^2}. \quad (1)$$

where $\mathbf{q} = \mathbf{p} - \mathbf{k}$ and $E_n - E_m$ are, respectively, the momentum and frequency the electrons exchange upon scattering, ε_∞ and ε_0 are high-frequency and static dielectric constants, ω_L is the LO-phonon frequency, and $|V_{\mathbf{q}}|^2 = 4\pi\alpha(\omega_L/q)^2(2m_b\omega_L)^{-1/2}$ is the squared modulus of the electron-phonon interaction amplitude with the band mass m_b and the electron-phonon coupling constant $\alpha = e^2(m_b/2\omega_L)^{1/2}(1/\varepsilon_\infty - 1/\varepsilon_0)$. In a *multimode* polar crystal with n optical-phonon branches,

like SrTiO₃, the matrix element (1) is extended in a straightforward way:

$$\Gamma(\mathbf{p}, E_n | \mathbf{k}, E_m) = \frac{4\pi e^2}{\varepsilon_\infty q^2} - \sum_{j=1}^n \frac{2\omega_{L,j} |V_{\mathbf{q},j}|^2}{\omega_{L,j}^2 + (E_n - E_m)^2}. \quad (2)$$

where $V_{\mathbf{q},j}$ is the electron-phonon interaction amplitude for a j -th LO-phonon branch. The partial coupling strengths for any phonon branch in a continuum approach for the electron-phonon interaction can be determined as described in Refs. [30, 13]. The amplitudes of the electron-phonon interaction for a large (Fröhlich) polaron in a multimode crystal are:

$$|V_{\mathbf{q},j}|^2 = \frac{4\pi e^2}{q^2} \left(\frac{\partial \varepsilon(\omega)}{\partial \omega} \right)^{-1} \Bigg|_{\omega=\omega_{L,j}}, \quad (3)$$

where $\varepsilon(\omega)$ is a dielectric function for a crystal.

Let us substitute in (3) the frequently used model dielectric function for a multimode polar crystal [30, 31]:

$$\varepsilon(\omega) = \varepsilon_\infty \prod_{j=1}^n \left(\frac{\omega^2 - \omega_{L,j}^2}{\omega^2 - \omega_{T,j}^2} \right), \quad (4)$$

whose zeros and poles correspond to the LO and TO phonon frequencies $\{\omega_{L,j}, \omega_{T,j}\}$, respectively. This dielectric function is the result of the extension of the Born-Huang approach [32] to multimode polar crystals. A particular consequence of (4) is the extension of the Lydanne-Sachs-Teller (LST) relation: $\varepsilon_\infty/\varepsilon_0 = \prod_{j=1}^n (\omega_{T,j}^2/\omega_{L,j}^2)$. One can explicitly check the exact analytic equality:

$$1 - \sum_{j=1}^n \left(1 - \frac{\omega_{T,j}^2}{\omega_{L,j}^2} \right) \prod_{j' \neq j} \left(\frac{\omega_{L,j}^2 - \omega_{T,j'}^2}{\omega_{L,j}^2 - \omega_{L,j'}^2} \right) = \frac{\varepsilon_\infty}{\varepsilon_0}. \quad (5)$$

In the antiadiabatic case, as assumed in Ref. [17], $\omega_{L,j} \gg |E_n - E_m|$ and hence one can omit $|E_n - E_m|$ in the denominator of the phonon Green function in (2). Accounting for (5), the matrix element of the effective electron-electron interaction provided by the interplay of the Coulomb repulsion and the LO-phonon-mediated attraction in the antiadiabatic limit is reduced to the expression, *which is the same for single-mode and multimode crystals*:

$$\Gamma(\mathbf{p}, E_n | \mathbf{k}, E_m) |_{\omega_{L,j} \gg |E_n - E_m|} = \frac{4\pi e^2}{\varepsilon_0 q^2}. \quad (6)$$

Thus the effective attraction in a multimode polar crystal in the antiadiabatic limit results in the replacement of ε_∞ to ε_0 where ε_0 accounts for the polarization due to *all* phonon modes. After this partial compensation of the Coulomb repulsion, *no more LO phonons remain to*

provide additional attraction. Moreover, beyond the antiadiabatic limit, when we do not neglect $(E_n - E_m)^2$ in the denominator of (2), the sum over LO-phonon modes in (2) becomes even smaller. Thus, as long as the LO-phonon-mediated effective electron-electron interaction is modeled by a *static* two-particle potential, it is not sufficient to provide superconductivity in a polar (both single-mode and multimode) crystal. The physical reason for this conclusion is quite transparent. In the antiadiabatic limit, the dielectric response of a crystal on the electron is the same as on a static charge, resulting in the static dielectric function. The static dielectric function in the long-wavelength limit must be positive from the stability condition. Therefore the total effective interaction remains repulsive. Also in layered structures [28], the phonon-mediated attraction in the antiadiabatic limit results in static dielectric image forces which cannot overcome the Coulomb repulsion. We can conclude that an effective LO-phonon-mediated attraction between electrons in polar crystals can overcome the Coulomb repulsion only when taking into account a *dynamic* electron-phonon response through the frequency-dependent dielectric function [18]. Moreover, the dynamical electron-electron interaction can *cooperate* with the electron-phonon pairing interaction [25, 26].

We consider the general case for the ratios of the LO-phonon energies to the thermal and Fermi energies, without assuming adiabatic or antiadiabatic limits. The calculation accounting for a multiband structure of the conduction band is based on the gap equation from Ref. [15] for the gap parameter $\Delta_\lambda(\mathbf{k})$ (neglecting the interband Josephson coupling, because it is not known and apparently does not strongly influence the overall magnitude of T_c):

$$\Delta_\lambda(\mathbf{p}) = -\frac{1}{(2\pi)^3} \int d\mathbf{k} \Delta_\lambda(\mathbf{k}) \frac{\tanh \frac{\beta|\varepsilon_{\mathbf{k},\lambda}|}{2}}{2|\varepsilon_{\mathbf{k},\lambda}|} \times \left[V_\lambda^0(\mathbf{p} - \mathbf{k}) + \frac{2}{\pi} \int_0^\infty d\Omega \frac{\text{Im} V_\lambda^R(\mathbf{p} - \mathbf{k}, \Omega)}{\Omega + |\varepsilon_{\mathbf{k},\lambda}| + |\varepsilon_{\mathbf{p},\lambda}|} \right], \quad (7)$$

where λ is the index of the subband of the conduction band, $\varepsilon_{\mathbf{k},\lambda}$ is the electron energy counted from the chemical potential, $V_\lambda^R(\mathbf{q}, \Omega)$ is the effective electron-electron interaction potential, and $V_\lambda^0(\mathbf{q})$ is its high-frequency limit. The effective interaction potential takes into account both the Coulomb and retarded phonon-mediated interactions, being expressed through the total dielectric function of the electron-phonon system $\varepsilon_\lambda^R(q, \Omega)$:

$$V_\lambda^R(\mathbf{q}, \Omega) = \frac{4\pi e^2}{q^2 \varepsilon_\lambda^R(\mathbf{q}, \Omega)}. \quad (8)$$

Here, $\varepsilon_\lambda^R(\mathbf{q}, \Omega)$ is the total dielectric function of the electron-phonon system for the λ -th band. We use the dielectric function accounting for multiple LO-phonon branches as treated in Ref. [13]. The total dielectric function (including both the lattice and electron polarization) is calculated within the random phase approximation (RPA).

The trial gap parameter is modeled by the function $\Delta_\lambda(\omega)$ depending on the energy. The integral over the electron momentum \mathbf{k} can be transformed to the integral with the density of states in the λ -th band $\nu_\lambda(\varepsilon)$:

$$\frac{1}{(2\pi)^3} \int d\mathbf{k} \dots = \frac{1}{4\pi} \int d\varepsilon \nu_\lambda(\varepsilon) \int d\omega \dots \quad (9)$$

and hence we arrive at the gap equation

$$\Delta_\lambda(\omega) = - \int_{-\varepsilon_F}^\infty \frac{d\omega'}{2\omega'} \tanh\left(\frac{\beta\omega'}{2}\right) K_\lambda(\omega, \omega') \Delta_\lambda(\omega') \quad (10)$$

with the kernel

$$K_\lambda(\omega, \omega') = \frac{\nu_\lambda(\omega')}{(4\pi)^2} \int d\omega \int d\omega' \left[V_\lambda^0(\mathbf{p}_\omega - \mathbf{p}_{\omega'}) + \frac{2}{\pi} \int_0^\infty d\Omega \frac{\text{Im} V_\lambda^R(\mathbf{p}_\omega - \mathbf{p}_{\omega'}, \Omega)}{\Omega + |\omega| + |\omega'|} \right]. \quad (11)$$

Here, the moments \mathbf{p}_ω for a given energy ω are restricted by the equation for an isoenergetic surface $\varepsilon_{\mathbf{p},\lambda} = \omega$.

The gap equation (10) provides the energy-dependent gap parameter, accounting then for a dynamic response of the electron-phonon system. It appears that the kernel function is always positive [16]. However, a significant frequency dependence of $K_\lambda(\omega, \omega')$ does allow for non-trivial solutions of the superconducting gap equation. These solutions come along with a significant variation of the order parameter $\Delta_\lambda(\omega)$ as a function of frequency, where a sign change of $\Delta_\lambda(\omega)$ can appear near the Fermi energy. This behavior of the gap parameter might be visible in tunneling experiments.

3 Discussion and summary

The novelty of the present study with respect to the preceding works consists in using the multimode dielectric function for SrTiO₃ with experimentally determined LO and TO frequencies and in using the multiband model for the electron conduction band with reliable band parameters corresponding to recent experimental [22] and theoretical [21] works on the band structure of SrTiO₃. For the numeric calculation, the

high-frequency dielectric constant $\varepsilon_\infty \approx 5.44$ and the LO and TO phonon frequencies in SrTiO₃ that we use are the same as those listed in our paper [13], taken from literature sources (no fitting). The only parameter which is not yet known definitely is the absolute deformation potential D for the electron – acoustic-phonon interaction. Here, as in our paper on superconductivity in a LAO-STO structure, we compare results for three physically reasonable values: $D = 3$ eV, $D = 4$ eV and $D = 5$ eV. The value $D = 4$ eV was reported in Ref. [23]. The value $D = 3$ eV is very close to that (2.87 eV) found in Ref. [24].

The electrons in the conduction band are described by the matrix Hamiltonian from Ref. [21]

$$H_{ij} = \delta_{i,j}\varepsilon_j(\mathbf{k}) + W_{ij}/2 \quad (12)$$

with the energies

$$\varepsilon_j(\mathbf{k}) = 4t_\pi \sum_{i \neq j} \sin^2\left(\frac{a_0 k_i}{2}\right) + 4t_\delta \sin^2\left(\frac{a_0 k_j}{2}\right), \quad (13)$$

where a_0 is the lattice constant. The matrix W

$$W = \begin{pmatrix} 2d & \xi & \xi \\ \xi & 2d & \xi \\ \xi & \xi & -4d \end{pmatrix} \quad (14)$$

describes the mixing of subbands within the conductivity band. We use the values of the band parameters t_δ, t_π, d, ξ from Ref. [21]: $t_\delta = 35$ meV, $t_\pi = 615$ meV, $\xi = 18.8$ meV and $d = 2.2$ meV.

Next, we take into account the fact that even for the highest concentration of electrons at which the superconductivity in n -doped SrTiO₃ is observed (about $n_0 \approx 4 \times 10^{20}$ cm⁻³), the Fermi energy of electrons (counted from the bottom of the lowest band) is $E_F \sim 0.1$ eV, which is very small with respect to the half-width of the conduction band (~ 2.5 eV). Therefore we can use the parabolic approximation for each subband determining the parameters from the tight-binding model [21] described above. Following Ref. [15], the band mass used in the present calculation is the density-of-state band mass $m_D = (m_{xx}m_{yy}m_{zz})^{1/3}$. The values of $m_{D,\lambda}$ appear to be different for different λ : $m_{D,1} \approx 0.669m_e$, $m_{D,2} \approx 0.622m_e$, and $m_{D,3} \approx 0.595m_e$, where m_e is the electron mass in vacuum. The inverse-averaged band mass [determined as $m_b^{-1} = (m_{xx}^{-1} + m_{yy}^{-1} + m_{zz}^{-1})/3$] is with high accuracy one and the same for three bands: $m_b \approx 0.593m_e$.

The critical temperatures for the superconducting phase transition on the SrTiO₃/LaAlO₃ interface have been calculated in Ref. [16]. In Fig. 1, we show the critical temperatures vs the two-dimensional electron concentration. The results are compared to the experimental data of Refs. [2,3,4].

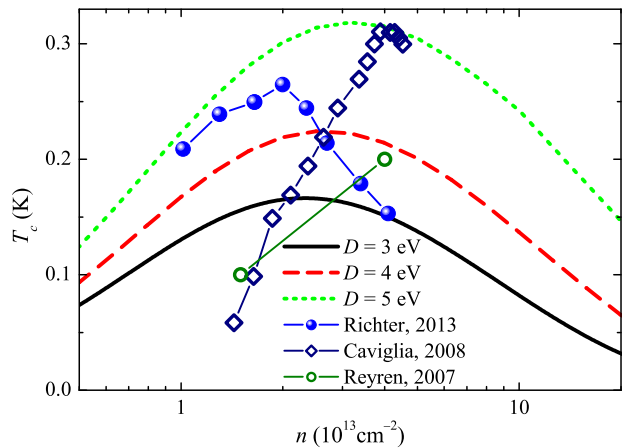


Fig. 1 Critical temperature for the superconducting phase transition for the electron gas on the SrTiO₃/LaAlO₃ interface, compared to the experimental data of Refs. [2,3,4].

The numeric results for the critical temperatures in bulk strontium titanate as a function of the electron concentration are shown in Fig. 2. When neglecting the Josephson interband coupling, the actual critical temperature is determined as the highest T_c of the solutions of the gap equation (10) for three subbands of the conduction band. These particular solutions are shown in the figure by dashed curves, and the resulting T_c for each D are shown by the curves with full dots.

Qualitatively, the measured critical temperatures in different experiments, both for bulk strontium titanate and for its interface, lie in the same range of the carrier concentrations and have the same range of magnitude. However, there exists a significant discrepancy between different experimental data. These discrepancies of the experimental results has a transparent explanation. The thermal energy is very small with respect to the Fermi energy of the electrons and the LO-phonon energies. Therefore the critical temperatures can be very sensitive to relatively small difference of the material parameters of the experimental samples. Thus even a relatively small change of these parameters can then lead to a significant change of the critical temperature. Moreover, experimental data are obtained with some numeric inaccuracy which also influences the results.

The obtained density dependence of the critical temperatures in n -doped SrTiO₃ is in line with the existing experimental data [14,27] without fitting. Moreover, the calculated critical temperatures, as well as the experimental results, correspond to the physical picture of the multiband superconductivity in strontium titanate. We can see that the theoretical model based on the dielectric function formalism adequately describes

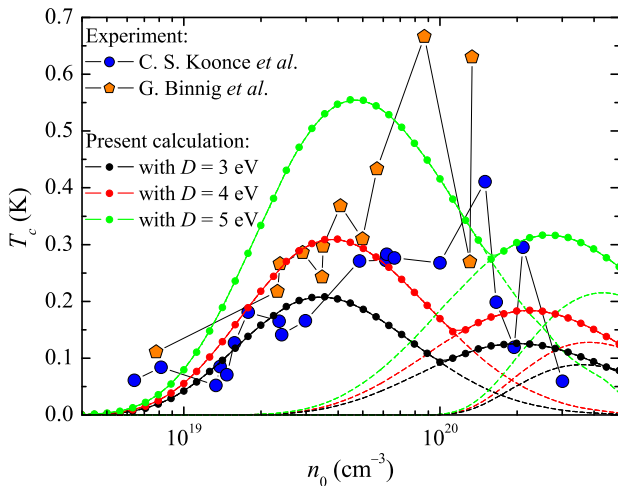


Fig. 2 Critical temperature for the superconducting phase transition in n -doped SrTiO_3 as a function of the carrier density. The results of the present calculation for three values of the deformation potential D are shown by full dots. The calculated critical temperatures are compared with the experimental data [14,27] shown by symbols.

the superconductivity in SrTiO_3 both qualitatively and quantitatively.

In summary, the dielectric function method provides thusfar the most reliable explanation of superconductivity in strontium titanate, both in bulk and at its interface. In the dielectric response of the electron-phonon system, all phonon branches are taken into account. The interplay between the dynamic screening of the Coulomb interaction, as described by the pairing kernel function $K_\lambda(\omega, \omega')$ and the values of the Fermi energy ε_F can provide a non-monotonic dome-shape of the critical temperature both in bulk SrTiO_3 and on the $\text{SrTiO}_3/\text{LaAlO}_3$ interface, being in line with experimental data. Despite the apparent uncertainty of the experimental results on the critical temperatures, the theoretical treatment of the superconducting phase transition in bulk strontium titanate and on the $\text{SrTiO}_3/\text{LaAlO}_3$ interface leads to qualitative agreement with experiment without fitting material parameters. The calculated critical temperatures, as well as the experimental results, agree with the physical picture of multiband superconductivity, and support the hypothesis that the mechanism of superconductivity in SrTiO_3 and on the $\text{SrTiO}_3/\text{LaAlO}_3$ interface is provided by the electron - optical-phonon interaction.

Acknowledgements This work is supported by the Flemish Research Foundation (FWO-VI), project nrs. G.0115.12N, G.0119.12N, G.0122.12N, G.0429.15N, by the Scientific Research Network of the Research Foundation-Flanders, WO.033.09N, and by the Research Fund of the University of Antwerp.

References

1. A. Ohtomo and H. Y. Hwang, *Nature (London)* **427**, 423-426 (2004).
2. N. Reyren, S. Thiel, A. Caviglia, L. Fitting Kourkoutis, G. Hammerl, C. Richter, C. Schneider, T. Kopp, A.-S. Rüetschi, D. Jaccard, M. Gabay, D. Müller, J.-M. Triscone, and J. Mannhart, *Science* **317**, 1196-1199 (2007).
3. A. Caviglia, S. Gariglio, N. Reyren, D. Jaccard, T. Schneider, M. Gabay, S. Thiel, G. Hammerl, J. Mannhart, and J.-M. Triscone, *Nature (London)* **456**, 624-627 (2008).
4. C. Richter, H. Boschker, W. Dietsche, E. Fillis-Tsirakis, R. Jany, F. Loder, L. F. Kourkoutis, D. A. Müller, J. R. Kirtley, C. W. Schneider, and J. Mannhart, *Nature* **502**, 528-531 (2013).
5. H. Boschker, C. Richter, E. Fillis-Tsirakis, C. W. Schneider, and J. Mannhart, *Sci. Rep.* **5**, 12309 (2015).
6. E. Fillis-Tsirakis, C. Richter, J. Mannhart and H. Boschker, *New J. Phys.* **18**, 013046 (2016).
7. L. Li, C. Richter, J. Mannhart, and R. C. Ashoori, *Nature Phys.* **7**, 762-766 (2011).
8. J. A. Bert *et al.*, *Nature Phys.* **7**, 767-771 (2011).
9. D. A. Dikin *et al.*, *Phys. Rev. Lett.* **107**, 056802 (2011).
10. A. D. Caviglia *et al.*, *Phys. Rev. Lett.* **104**, 126803 (2010).
11. Z. Zhong, A. Tóth, and K. Held, *Phys. Rev. B* **87**, 161102 (2013).
12. X. Lin, Z. Zhu, B. Fauqué, and K. Behnia, *Phys. Rev. X* **3**, 021002 (2013).
13. J. T. Devreese, S. N. Klimin, J. L. M. van Mechelen, and D. van der Marel, *Phys. Rev. B* **81**, 125119 (2010).
14. C. S. Koonce, M. L. Cohen, J. F. Schooley, W. R. Hosler, and E. R. Pfeiffer, *Phys. Rev.* **163**, 380-390 (1967).
15. Y. Takada, *J. Phys. Soc. Jpn.* **49**, 1267-1275 (1980).
16. S. N. Klimin, J. Tempere, J. T. Devreese and D. van der Marel, *Phys. Rev. B* **89**, 184514 (2014).
17. L. P. Gor'kov, "Phonon mechanism in the most dilute superconductor: n -type SrTiO_3 ", *arXiv:1508.00529* (2015).
18. D. A. Kirzhnits, E. G. Maksimov and D. I. Khomskii, *J. Low Temp. Phys.* **10**, 79-93 (1973).
19. Y. Takada, *J. Phys. Soc. Jpn.* **45**, 786-794 (1978).
20. J. L. M. van Mechelen, D. van der Marel, C. Grimaldi, A. B. Kuzmenko, N. P. Armitage, N. Reyren, H. Hagemann, and I. I. Mazin, *Phys. Rev. Lett.* **100**, 226403 (2008).
21. D. van der Marel, J. L. M. van Mechelen, and I. I. Mazin, *Phys. Rev. B* **84**, 205111 (2011).
22. W. Meevasana *et al.*, *New J. Phys.* **12**, 023004 (2010).
23. A. Janotti, B. Jalan, S. Stemmer, and C. G. Van de Walle, *Appl. Phys. Lett.* **100**, 262104 (2012).
24. A. N. Morozovska, E. A. Eliseev, G. S. Svechnikov, and S. V. Kalinin, *Phys. Rev. B* **84**, 045402 (2011).
25. R. Akashi and R. Arita, *Phys. Rev. Lett.* **111**, 057006 (2013).
26. A. J. Leggett, *Proc. Natl Acad. Sci. USA* **96**, 8365-8372 (1999).
27. G. Binnig, A. Baratoff, H. E. Hoernig, and J. G. Bednorz, *Phys. Rev. Lett.* **45**, 1352-1355 (1980).
28. L. P. Gor'kov, *Phys. Rev. B* **93**, 060507(R) (2016).
29. J. Bardeen and D. Pines, *Phys. Rev.* **99**, 1140-1150 (1955).
30. Y. Toyozawa, in: *Polarons in Ionic Crystals and Polar Semiconductors*, North-Holland, Amsterdam (1972), pp. 1 - 27.
31. R. Zheng, T. Taguchi, and M. Matsuura, *Phys. Rev. B* **66**, 075327 (2002).
32. M. Born and K. Huang, *Dynamical Theory of Crystal Lattices* (Clarendon, Oxford, 1954).